Development of a high-speed, high fill-factor phase-only spatial light modulator

Vern Shrauger[1] and Cardinal Warde[2]
Optron Systems, Inc., 3 Preston Court, Bedford, MA 01730

ABSTRACT

This paper demonstrates a MEMS (microelectromechanical systems) technology for the fabrication of a high-speed, phase-only spatial light modulator (SLM). An independently developed low temperature MEMS process for the vertical integration of MEMS directly onto VLSI substrates is presented. The low temperature process enables the use of standard VLSI wafers integrated with MEMS at the post-process level.

A MEMS structure has been demonstrated that produces polarization-independent pixel-wise pure-piston phase delay with optically flat micromirrors fabricated on a mock VLSI substrate as a proof-of-concept device. The gray-scale phase modulation offers $-\pi$ to $+\pi$ dynamic range in the ultraviolet to near infrared spectrum without mechanical contact. Pixel sizes as small as 40 microns with 86% fill-factor have been demonstrated. In addition to high fill-factor, micromirror reflectivity exceeding 95% that significantly minimizes optical insertion loss and enables high power operation has also been confirmed with this novel process. Furthermore, single-pixel operating speeds in excess of 100 kHz have been verified. The high operating speeds enable electrically addressed framing rates that are limited by the electronic interface bandwidth as opposed to the optical modulating element. We are presently fabricating a monolithically integrated phase-only modulator on CMOS VLSI creating a compact, lightweight, low-cost SLM. The resulting 256x256, 4 kHz framing rate, gray-scale phase-only SLM has applications including adaptive optics, high-speed optical correlators, phased array beam steering and diffractive beam forming.

Keywords: spatial light modulator, phase-only modulation, light valve, MEMS, MOEMS, adaptive optics, optical signal processing

1. INTRODUCTION

Spatial light modulators (SLMs) [1-3] or light valves as they are often called, are the building blocks of optical information processors. These devices modify the polarization, phase, and/or amplitude of a readout light beam as a function of space and time in response to an electrical or optical drive signal, which may also be two-dimensional.

Progress in the development of optical information processing systems is being impeded by the lack of high performance spatial light modulators (SLMs). At present one can find a few SLMs on the market that modulate either the amplitude or the phase (or both) of a readout light beam at framing rates exceeding 1 kHz [4]. Phase-only spatial light modulators however are of special interest in optical signal processing systems. For example, it is well known that in the classical two-lens correlator, phase-only matched spatial filters outperform their amplitude and fully complex counterparts. In addition, the joint transform correlator could experience true real time operation if such a high-speed, high resolution, phase-only spatial light modulator were available. A high-speed phase-only SLM would significantly improve the throughput of correlators used for optical signal and image processing.

Recently, microelectromechical systems (MEMS) based phase-only SLMs have been developed and used for adaptive optics applications [5-7]. In addition, much recent attention has been paid to MEMS for optical applications, or MOEMS (micro-opto-electromechanical systems) [8]. In the majority of the MOEMS applications, surface [9-10] or bulk micromachining processes are employed to create such devices. Most of these micromachining processes do not incorporate VLSI (very large scale integration) electronics into the process flows because of thermal budget and material constraints. The few processes that do include VLSI electronics, such as the SUMMiT V process [10], do so in a laterally integrated fashion. By including VLSI electronics within a MEMS process, full system integration from MEMS drive and sense to external interface

[1] Present Address: Axiowave Networks, Inc., 100 Nickerson Road, Marlborough, MA 01752, vshrauger@axiowave.com
[2] Permanent Address: Room 13-3102, Massachusetts Institute of Technology, Cambridge, MA 02139, warde@mtl.mit.edu

© 2001 SPIE · 0277-786X/01/$15.00

electronics is possible. Unfortunately for SLMs, lateral integration of electronics severely limits pixel fill-factors because of the significant real estate consumed by the electronics.

To address the fill-factor issue for SLMs, Texas Instruments (TI) developed a metals-over-VLSI process for their DLP (digital light processor) which is found in many of the present state-of-the-art projection displays. This device tilts a MEMS mirror in a binary fashion, and with spatial filtering, generates a high-contrast binary amplitude display, which is modulated in time to generate color images [11]. The present TI process vertically integrates MEMS mirrors over a CMOS VLSI substrate. This particular process requires significant process control over the metals employed to achieve good quality mirror surfaces. We have developed an alternate approach to solve the vertical integration of MEMS over VLSI with greater tolerance to process variability. The developed process has been used in an effort to create a high-speed phase-only spatial light modulator presented here.

At present, the MEMS process has been demonstrated with a proof-of-concept device, which enabled phase-only evaluation with modulated grating connection of mirrors. By ganging many phase-only mirrors in alternating rows, a modulating grating of many phase elements was demonstrated. These gratings were modulated in excess of 100 kHz suggesting that SLMs limited by the bandwidth of electronic data transmission are possible. Optron Systems, Inc. is presently fabricating a prototype 128x128 phase-only SLM.

In Section 2, we briefly discuss the overall approach to our SLM device and the proof-of-concept demonstration. Additionally, some of the scanning electron micrographs (SEM) of the device at various stages in its fabrication and verification of the mirror surface flatness are presented. In section 3, the experimental characteristics of the actuated phase-only element are discussed. To demonstrate the proof-of-concept device, we configured the phase-only modulator as a grating and measured the zero order response, calculated the phase modulation depth and measured the frequency response. In section 4, the results are summarized and directions of future work at Optron Systems, Inc. are presented.

2. PROOF-OF-CONCEPT DEVICE

Ultimately, we will build a phase-only SLM on a planarized VLSI wafer. To demonstrate a proof-of-concept spatial light modulator, we have used an insulated silicon wafer to mimic our base VLSI substrate. A cross-sectional view of the phase-only modulator is shown in Figure 1.

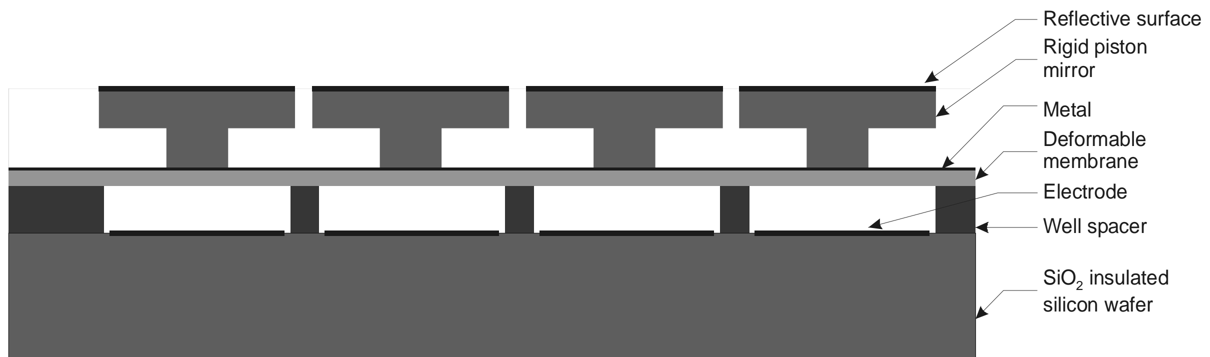

Figure 1: Proof-of-concept MEMS based phase-only modulator built on a blank silicon wafer.

The prototype modulator employed interdigitated row/column addressing. On top of this wafer, we patterned the lower electrode structure and the first sacrificial layer prior to the deposition of the well spacer structural material. With the well spacers in place, we deposited a deformable membrane and metalization layer, which acts as the mechanical actuator to vertically move the piston structure. Atop the actuator, we deposited and patterned a second sacrificial layer to mold the piston structure. To create the rigid piston, a structural material is deposited onto the sacrificial mold and its top surface is planarized to form the optically flat reflector. The reflective layers are applied following the planarization step. For this proof-of-concept effort, we employed a metallic reflector. The individual mirror pistons are pixilated by patterning the mirror and the underlying structural material. To finally complete the moving device, the sacrificial material was removed.

A fully fabricated device structure as proposed in Figure 1 is shown in Figure 2. This figure represents the device without the final planarization step, which leaves a centrally dimpled surface on the reflector. SEM cross-sectional views of the 20 µm and 40 µm devices are shown in Figure 2a and Figure 2b, respectively. The reflector fill-factors are 72% and 86% respectively. For these particular devices, the central mirror posts are laterally misaligned. Both the reduced fill-factor and the slight lateral misalignment are due to the patterning limitations of the contact mask aligner that was used. With projection mask alignment, we expect fill-factors on the order of 90% and 95% respectively. Also in this figure, we observe that the mirror and its rigid substructure are firmly affixed to the underlying mechanical actuator. The mechanical actuator is a flat continuous membrane. The reflector substructure was cast thick to maintain a rigidly flat mechanical substrate for the reflective material. As discussed in Section 2.1, we analyzed the substructure curvature to predict surface warpage under residual stress conditions.

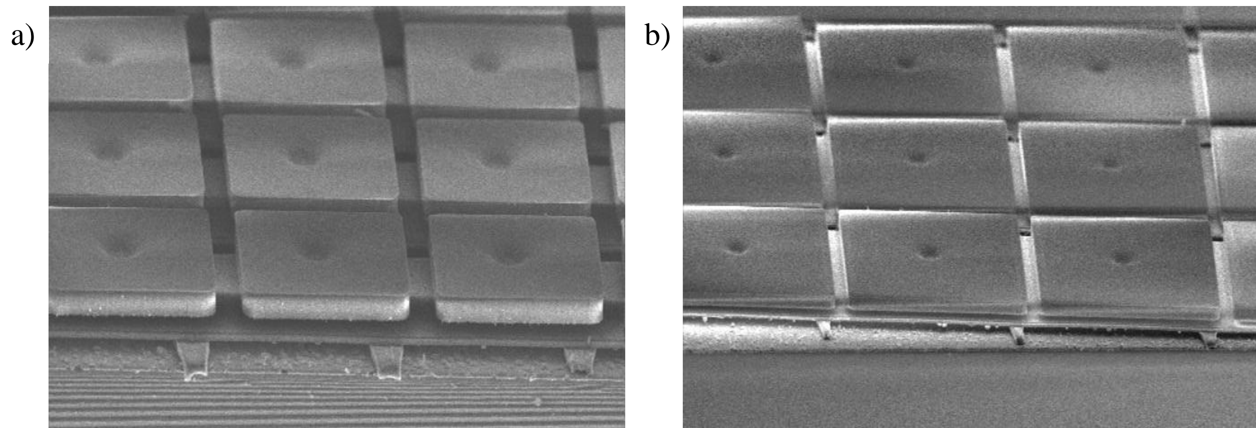

Figure 2: SEM cross-sectional view of the fully fabricated device on a) 20-µm and b) 40-µm pitch.

The central dimples in the reflector surface, as shown in Figure 2, are artifacts of an incomplete fabrication process. This dimpling effect is removed with a planarizing process. To confirm the piston structure and its surface quality, we fabricated a test wafer with this planarization step without the underlying membrane actuator. In Figure 3a, the 20 µm pitch (16.5 µm wide on 20 µm centers) reflector piston is observed to be extremely flat without the central dimple. Figure 3b shows an overturned piston structure illustrating the excellent pattern definition of the proposed piston. The background mirrors indicate there is a lack of any dimple in the reflector surface.

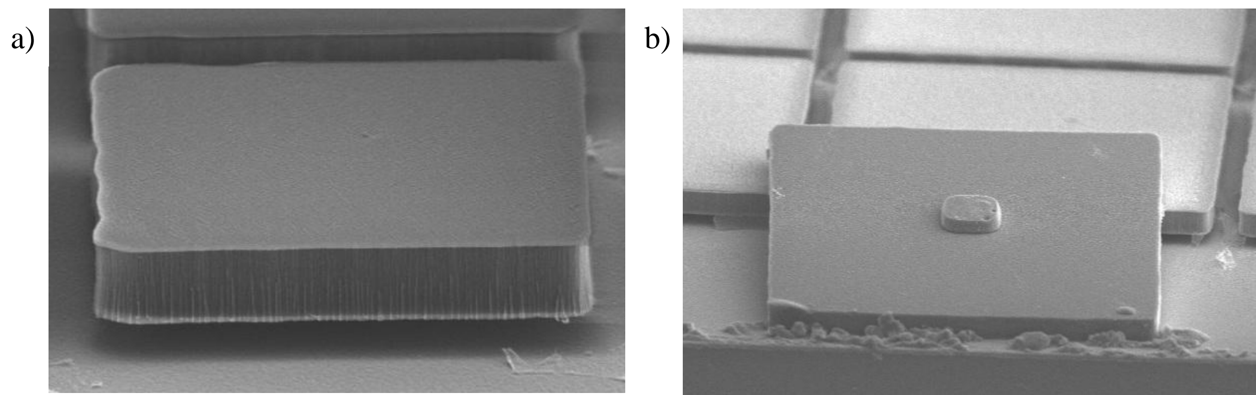

Figure 3: SEM image of a) a 20 µm reflector piston and b) an overturned 40 µm reflector piston indicating the central support post.

In a separately processed wafer lot, we completed the full device fabrication including the final planarization step. A Namarski phase contrast photograph of this 40-µm pitch device surface is shown in Figure 4. The device in this photograph was operated in excess of 2.5×10^{10} actuations in an air ambient without mirror degradation or delamination. As shown in this figure, the central dimple is still slightly apparent. In this case, the underlying post had a square cross-section approximately 9 µm on each side. As seen in this figure, the mirror surface is flat over the extent of the 40-µm mirror surface and there exists minimal variation from pixel to pixel within the array. This result indicates good array uniformity and minimal inter-pixel residual tilt.

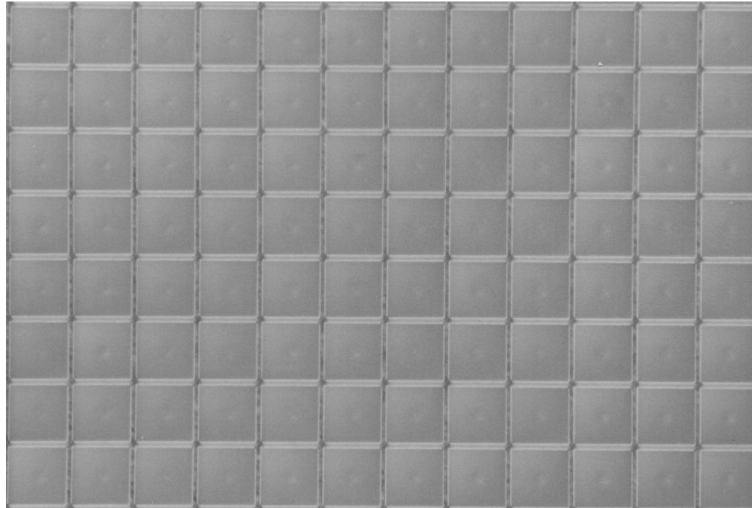

Figure 4: Namarski phase contrast photomicrograph of 40-μm pitch phase-only modulator.

2.1. Mirror Substructure

To verify the residual material stress acceptability, we have simulated a realistic reflective piston structure under two residual stress conditions, 2 MPa and 20 MPa. For this simulation, we built a 60 μm on a side square piston with a 6 μm on a side square post. The reflector substrate was specified as 2 μm thick and the post height (sacrificial layer thickness) was specified as 2 μm high. This structure is much larger than our targeted 20-μm goal, but was used to demonstrate optical flatness possible with much larger structures. We used MEMCAD [12] for the simulation, employed published material parameters, and assumed a uniform tensile stress distribution. The results of the simulations are shown in Figure 5. In this figure, the scale is grossly exaggerated to illustrate any flexure that occurs due to residual stress. The scales on the figures measure the displacement in microns. In both cases, the maximum flexure occurs at the corners of the piston shape. At these outlying corners, we are observing maximum bow of approximately 1 nm for a 2 MPa residual stress and approximately 10 nm deformation for a 20 MPa residual stress. In addition, we quickly re-ran the simulations with some realistic stress gradient in the z-direction and we did not observe significant variation from the results observed in Figure 5.

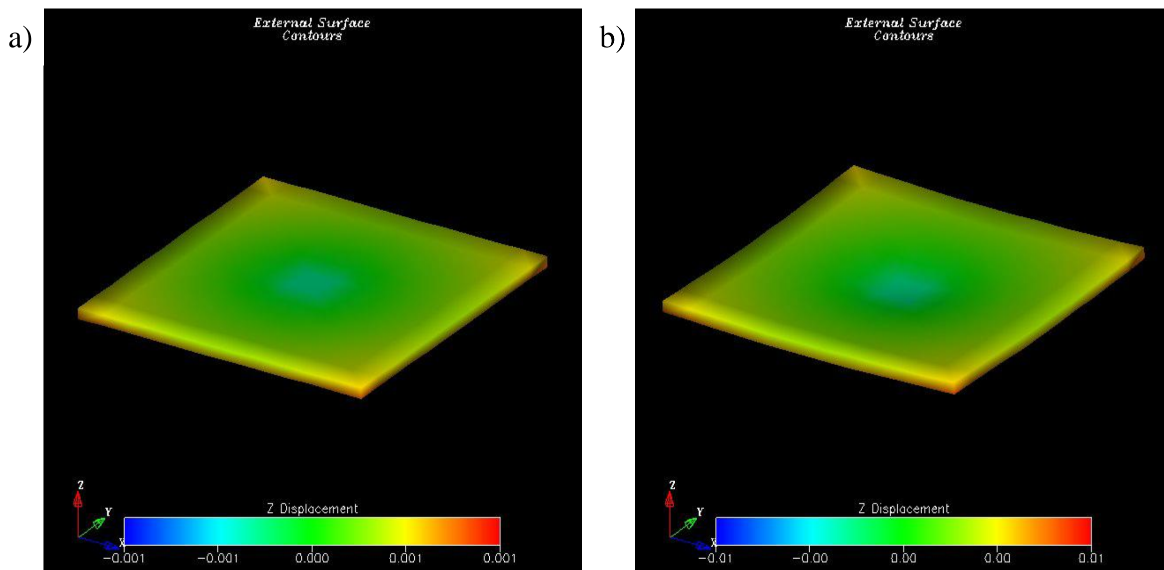

Figure 5: Reflector layer simulations as a function of tensile residual stress, a) 2 MPa and b) 20 MPa, in structural material, which defines the reflector piston.

As a result of our simulations, we see that a maximum deformation of 10 nm at the very corners of the 60-μm mirror surface under worst-case residual stress conditions will not significantly affect the inter-pixel phase flatness of the phase-only SLM. This indicates that the 20-μm or 40-μm pixels will not be significantly affected by the presence of practical amounts of residual stress. To confirm this theoretical prediction, we fabricated a freestanding reflector substructure without the underlying mechanical actuator and released the substructure for analysis. A SEM of the 60-μm pitch (5-μm gap, 55-μm reflector surface) mirror structure is illustrated in Figure 6. The reflector substructure is 2.5 μm thick and the buried reflector post is 8 μm on a side 2 μm high. As indicated in this figure, the suspended T structure is flat as predicted. This confirmation validates our materials choice and specifications for the 20-μm and pixel phase-only modulator.

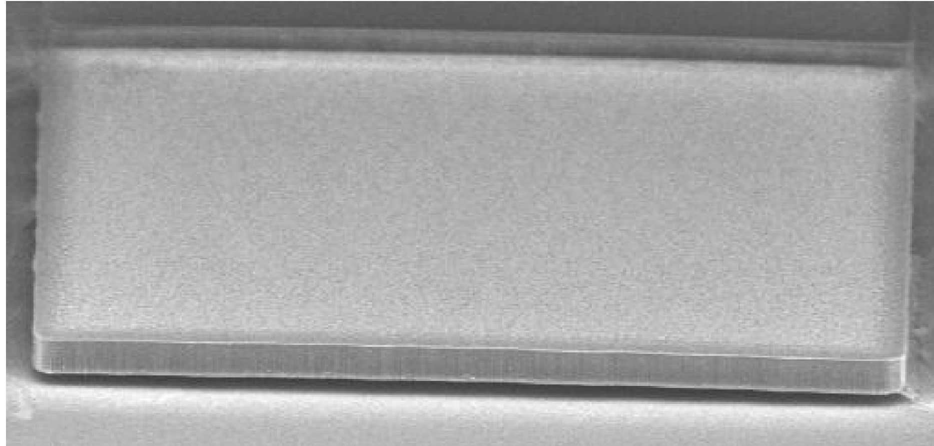

Figure 6: Experimentally released 60 μm reflector piston without underlying topography.

3. EXPERIMENTAL RESULTS

3.1. Phase Modulation

To verify the electrical operation of the device, as shown in Figure 4, we first measured the continuity between the upper and lower electrode and confirmed an open circuit. Our fabrication process has not produced any devices that were shorted. To characterize the dynamic mechanical and optical properties we applied an electric field to observe the mechanical motion of the released device and viewed the device diffraction through a spatial filter. Our test devices were designed with interdigitated rows and ganged columns so that we could drive the ganged mirror array as a reflective linear grating. Operating in this mode, the normalized measured amplitude in the zero-order diffraction spot is proportional to

$$A = 1 - \sin^2 \frac{2\pi d}{\lambda},$$

where d is the displacement of the mirror as operated in grating mode, and λ is the wavelength of operation. With this relation, the mirror displacement as a function of applied voltage can be determined by observing the zero-order light reflected off of the phase modulator driven as a grating device.

To measure the zero-order diffraction of the phase-only modulator, we used an unfiltered HeNe laser, 632.8 nm wavelength, transmitting through a beam splitter to illuminate the proof-of-concept phase modulator. We observed the zero-order reflection off the MOEMS device after a beam splitter and through an iris so as to observe only the zero order power. We used a high-speed photodiode and amplifier combination with sub-microsecond response time to measure the modulator response as actuated in an air ambient. The zero-order diffraction as a function of applied voltage is indicated in Figure 7. These data were taken using a square-wave drive signal at 50 kHz. As seen in this figure, a half-wave voltage, where destructive interfere occurs, of 58V was measured. We could not drive the device to the full-wave voltage because the single needle probe contact area was so small the contact would fail above 65V. From this curve, we employed the theoretical relations above to plot the displacement as a function of the applied voltage.

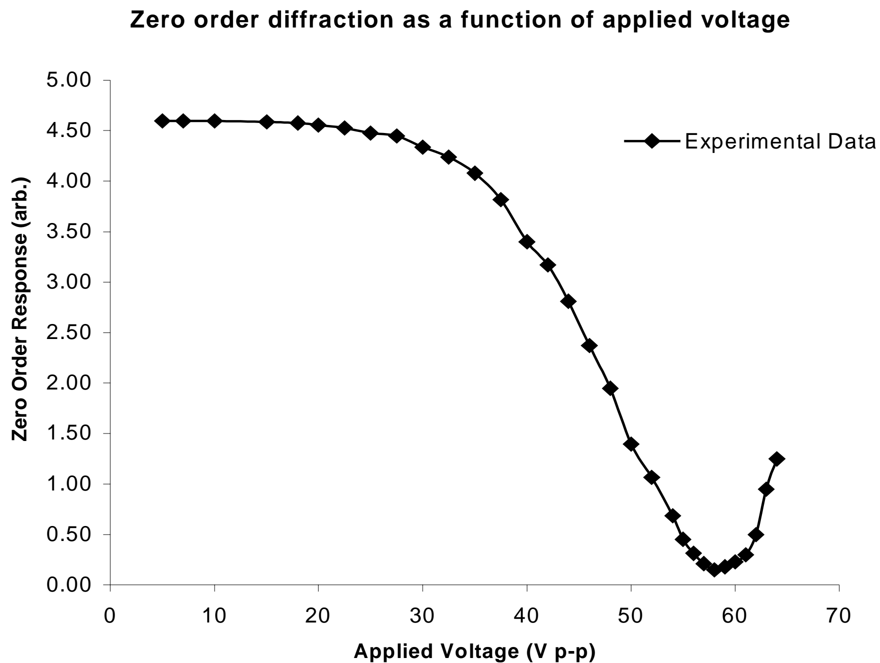

Figure 7: Zero-order diffraction from a 40-µm pitch phase-only modulation device.

The displacement of the 40-µm pitch piston as a function of applied voltage is observed in Figure 8. This device was designed so as to avoid the snapdown of the mechanical actuator as the displacement exceeds one-third the gap. For full-wave actuation, the vertical displacement would be 0.316-µm at the HeNe wavelength. In this displacement as a function of applied voltage plot, we have shown the experimental data and a best-fit curve. The best-fit curve indicates an approximate parabolic shape as would be expected for the electrostatic pull down of a parallel plate capacitor, where displacement is proportional to V^2.

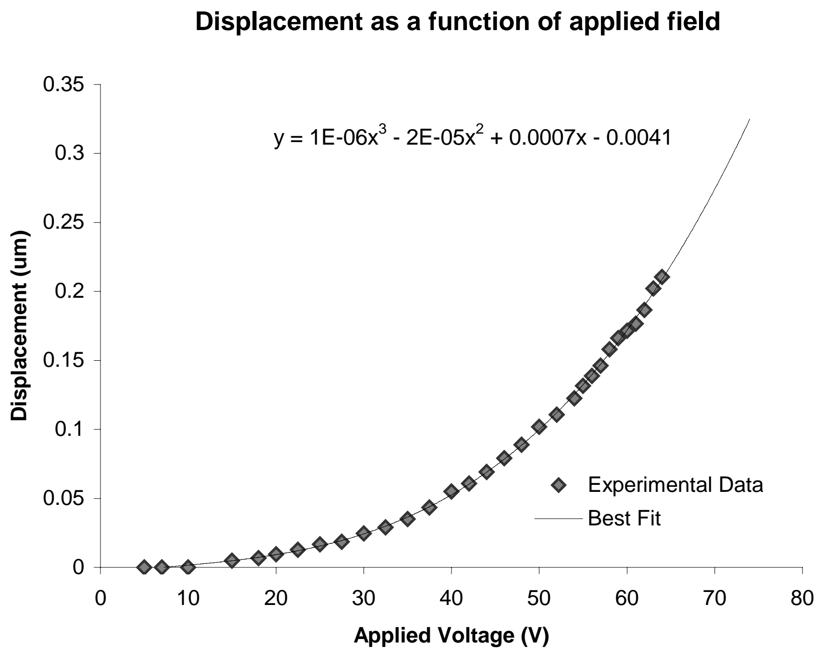

Figure 8: Displacement as a function of voltage for 40-µm pitch phase-only modulator.

3.2. Dynamic Response

To characterize the dynamic response of the phase modulator, we drove the phase modulator with square wave excitations. The oscilloscope traces of the zero-order diffraction responses when the device was driven in an air ambient are shown in Figure 9. In this figure, the phase modulator dutifully follows the input signal with a growing phase delay on the rising edge of the input signal as apparent in Figure 9b. In this figure, the upper trace indicates the input signal, and the lower trace indicates the photodetector/amplifier response.

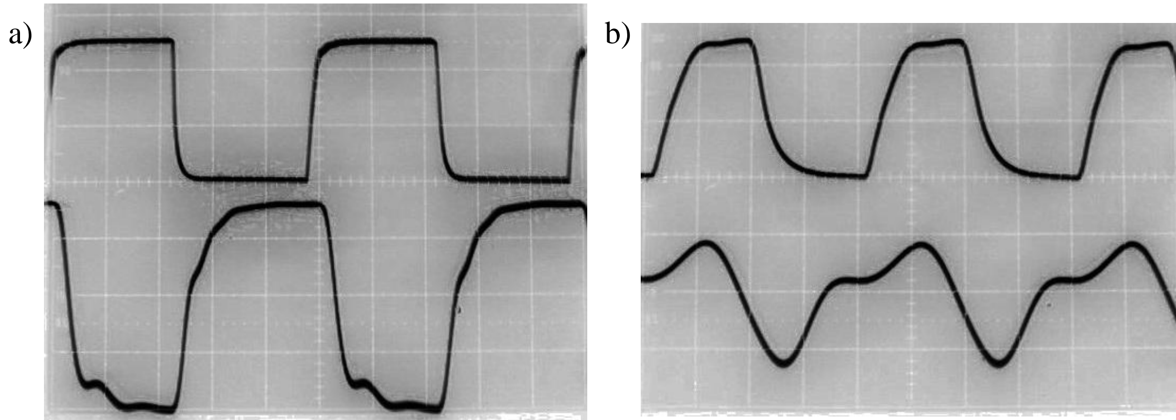

Figure 9: 40 μm pitch phase-only modulator driven with a 50V p-p input (upper trace), operating in an air ambient, and at a) 100 kHz (2 μs/div) and b) 500 kHz (500 ns/div).

In addition to measuring the displacement as a function of applied voltage for the phase-only modulator, we observed the frequency response when the device was operated in an air ambient. We have plotted the 40-μm pitch phase-only modulator frequency response in Figure 10. This measurement was taken by sweeping the frequency of a square wave input. The 3-dB point of this curve occurred at 500 kHz, which is approximately 300 kHz below the 3-dB point of the mechanical actuator, which does not incorporate the reflector substructure. This is due to the fact that a mirror mass is now loading the actuation of the underlying mechanical member. In the future, this measurement will be performed with a sine wave sweep to further characterize the resonant modes of the phase modulator.

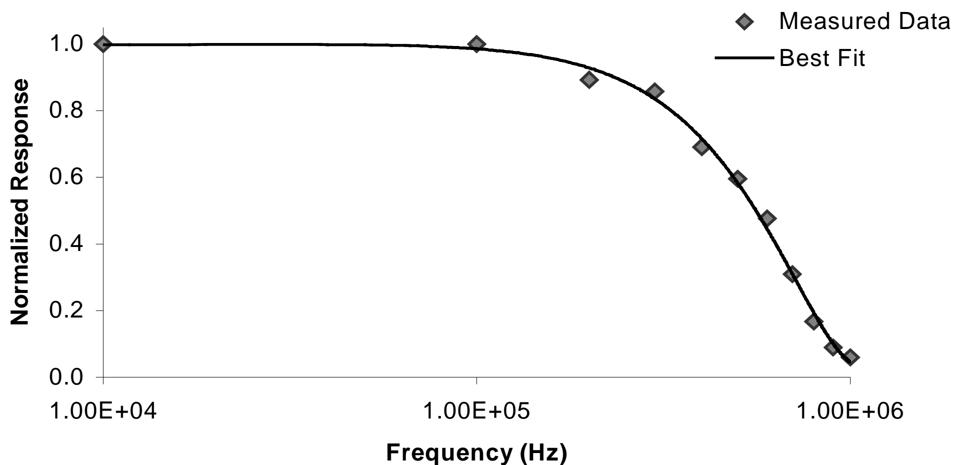

Figure 10: Frequency response of the 40-μm pitch phase-only modulator operating in an air ambient.

4. CONCLUSIONS AND FUTURE WORK

We have demonstrated the feasibility of a high-speed, MEMS based, phase-only spatial light modulator with a proof-of-concept device. We successfully developed a low-temperature MEMS process that is fully compatible with over-VLSI post-processing. This process includes materials routinely used in the semiconductor industry and could be directly integrated into an existing VLSI process line with the addition of 4 mask layer steps. The process was developed for post-process integration so that CMOS VLSI circuits could be subcontracted. The MEMS process was successfully demonstrated on dummy passivated silicon wafers. Several device structures were studied with the smaller devices indicating the best planarity. We have built 20, 40 and 60-μm pitch proof-of-concept devices. With minor device modifications, the operating voltages observed are within the voltage range achievable with high-voltage (50V) CMOS VLSI. With the measured experimental results, we expect 8-bits of phase resolution over the full-wave modulation range. We have demonstrated 100 kHz full modulation of the phase-only elements indicating that a high-speed SLM limited only by the addressing electronics will be possible.

Optron Systems, Inc. is presently engaged in the development of the prototype MEMS phase-only modulator over CMOS VLSI. Our prototype is targeted toward 128x128 SLM with 8-bit phase resolution at a 10 kHz and above framing rate. The present MEMS device structure will be optimized to minimize the driving voltage for full-wave operation.

ACKNOWLEDGEMENTS

We would like to thank Dennis Ward, Miriam Young and Wayne Price for their significant support during the fabrication effort. Dr. Nelsimar Vandelli, of Microcosm Technologies, Inc. for the helpful MEMCAD simulations. This work was supported in part by the Office of the Secretary of Defense/Air Force Research Laboratory, Eglin Air Force Base, contract number: F08630-00-C0002 and by the US Army Aviation & Missile Command, Redstone Arsenal, contract number: DAAH01-00-C-R083.

REFERENCES

1. S. Esener, J. L. Horner and K. M. Johnson, Guest Editors, Special issue of Applied Optics on Spatial Light Modulators and their Applications, Vol. 31, 1992.
2. U. Efron, A. D. Fisher and C. Warde, Guest Editors, Special Issue of Applied Optics on Spatial Light Modulators for Optical Information Processing, Vol 28, 1989.
3. C. Warde, and A. D. Fisher, "Spatial Light Modulators: Applications and Functional Capabilities", in Optical Signal Processing, J. Horner, Editor, Academic, 1987.
4. "Microdisplays, 2-dimensional spatial light modulators", Boulder Nonlinear Systems, Inc., http://www.bnonlinear.com/products.htm#2-D arrays
5. G. Vdovin, "Micromachined adaptive mirrors", TU Delft, 12 December 1996, http://guernsey.et.tudelft.nl/tyson4/index.html
6. M.C. Roggeman, V.M. Bright, B.M. Welsh, S.R. Hick, P.C. Roberts, W.D. Cowan, J.H. Comtols, "Use of micro-electro-mechanical deformable mirrors to control aberations in optical systems: theoretical and experimental results," Opt. Eng. 36(5), 1326-1338 (1997).
7. T.G. Bifano, et.al. "Continuous-membrane surface micromachined silicon deformable mirror," Opt. Eng., 36(5) 1354-1360 (1997).
8. M. E. Motamedi, W.C. Wu, K.S.J. Pister, "Micro-opto-electromechanical devices and on-chip optical processing," Opt. Eng. 36(5) 1282-1297 (1997).
9. D.A. Koester, R. Mahadevan, K.W. Markus, "MUMPS Introduction and Design Rules", MCNC MEMS Technology Applications Center, 1994.
10. "SUMMiT V Technology", Sandia National Laboratories, Intelligent Micromachine Initiative, http://www.mdl.sandia.gov/micromachine/summit5.html
11. L.J. Hornbeck, "Multilevel digital micromirror device", US Patent and Trademark Office 5,583,688, 1996.
12. "MEMCAD", Microcosm Technologies, Inc.,http://www.coventor.com/products.html